Chapter

Flicker-Noise Spectroscopy Method in the Problem of Diagnosing the State of the Cardiovascular System

Abdullayev Namiq Tahir and Ahmadova Khadija Ramiz

Abstract

In the field of research of the cardiovascular system, mainly analysis methods that are strictly mathematically applicable to stationary signals are distinguished; however, nonstationary signals prevail in medical practice, the statistical properties of which vary with time. Often they consist of short-term high-frequency components, followed by long-term low-frequency components. Given this nature of bioelectric potentials, and in particular electrocardiographic signals, the most suitable for their analysis may be the nonlinear dynamics method with the calculation of quantitative characteristics of chaos. This possibility is presented by the flicker-noise spectroscopy method, which takes into account the intermittency effect in a complex dynamic system when sections of chaotic bursts and jumps alternate with relatively long sections of a laminar nature. The analysis of signals of such a dynamic nature is usually based on the use of flicker-noise spectroscopy.

Keywords: flicker-noise spectroscopy, electrocardiographic signals, analysis, intermittency, diagnostics

1. Introduction

The flicker-noise spectroscopy method is proposed as a general phenomenological (non-model) approach to the analysis of chaotic signals of different nature. The essence of flicker-noise spectroscopy is to give informational significance to the correlation relationships that are realized in sequences of signal irregularities—bursts, jumps, and kinks of derivatives of various orders—as carriers of information about changes occurring at each spatiotemporal level of the hierarchical organization of the dynamic system under study. The autocorrelation function $\psi(\tau)$ is used as a basic image for extracting information from complex signals in the flicker-noise spectroscopy method [1, 2].

To classify information, this function is not analyzed but some of its transformations ("projections"), such as power spectrum $S(f)$, where f is the signal frequency, and the difference moment ("transition structure function") $\Phi^{(2)}(\tau)$ of the second order. The information extracted from the analysis of dependencies $S(f)$ and $\Phi^{(2)}(\tau)$, built on the basis of time series $V(t)$, has the meaning of correlation times or parameters, characterizing the loss of correlation relationships ("memory") for the irregularities under consideration such as bursts and jumps.

Moreover, only irregularities of the type of jumps of dynamic variable $V(t)$ contribute to the formation of dependence $\Phi^{(2)}(\tau)$, and jumps and bursts (outbursts) of chaotic series $V(t)$ contribute to the formation of $S(f)$.

The solution to the problem of predicting the evolution of a complex system and, above all, the search for precursors (precursors) of catastrophic changes in it is associated with the most dramatic changes in dependencies $S(f)$ and $\Phi^{(2)}(\tau)$ $(p = 2, 3, \ldots)$ calculated on the basis of high-frequency and low-frequency components $V(t)$.

2. Splitting an electrocardiographic signal into low-frequency and high-frequency components

The behavior of the electrocardiographic signal, reflecting the functional state of the cardiovascular system, is quite complicated and has the character of randomness.

The most general form of evolution in dynamic variable $V(t_i)$ for the ith space–time level of the electrocardiographic signal is presented in the form of intermittency, when not all intervals on the time axis are informationally equivalent. Such dynamics of the electrocardiogram (ECG) is characterized (**Figure 1**) by relatively weak changes in the variable over relatively long time intervals—"laminar phases" with characteristic durations of T_i and sudden interruptions of such evolution by abrupt changes in the value of the dynamic variable in the short intervals of duration τ_i $(\tau_i < T_i)$.

Each such abrupt change in the values of a dynamic variable then ends up with values in the subsequent "laminar" section. The magnitude and duration of such jumps, surges, and "laminar" sections are specific for each of the cardiovascular systems, causing a certain contribution to the corresponding power spectrum.

In this case, the studied signal $V(t)$ is conveniently represented as the sum of the two terms: the singular term $V_S(t)$, which is formed only by bursts of the dynamic variable, and the regular term $V_R(t) = V(t) - V_S(t)$, which is formed after subtracting bursts from the presented signal and determined by the jumps of the dynamic variable and "laminar phases."

The analysis of the electrocardiogram shows that it corresponds to the described dynamics, when bursts in the form of QRS complexes alternate with rather small jumps in the form of P and T teeth and extended phases in the form of an isoline.

The information contained in $S(f)$ and $\Phi^{(2)}(\tau)$ is different, so in order to determine the adequate parameters of the structure under study, it is necessary to analyze the dependencies $\log S(f) = F(\log f)$ and $\log \Phi^{(2)}(\tau) = F(\log \tau)$.

Let $V(t)$ denotes the dynamic variable, characterizing the ECG signal. We apply the proposed method of splitting the dynamic signal into low-frequency $V_R(t)$ and

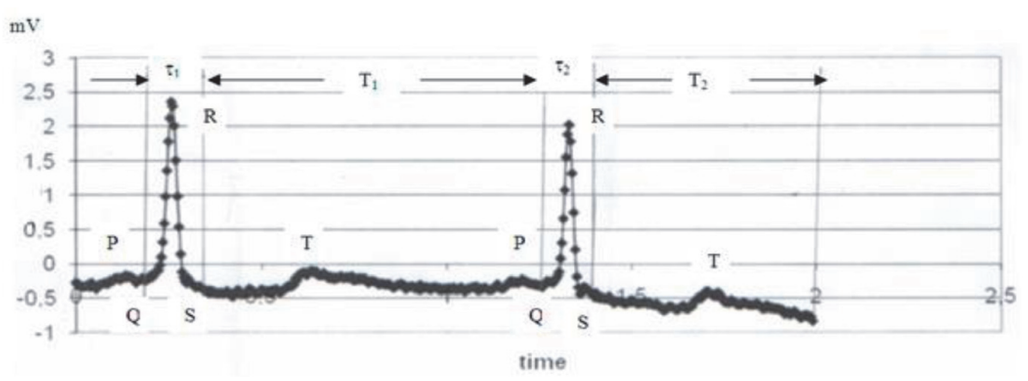

Figure 1.
The dynamics of the electrocardiogram.

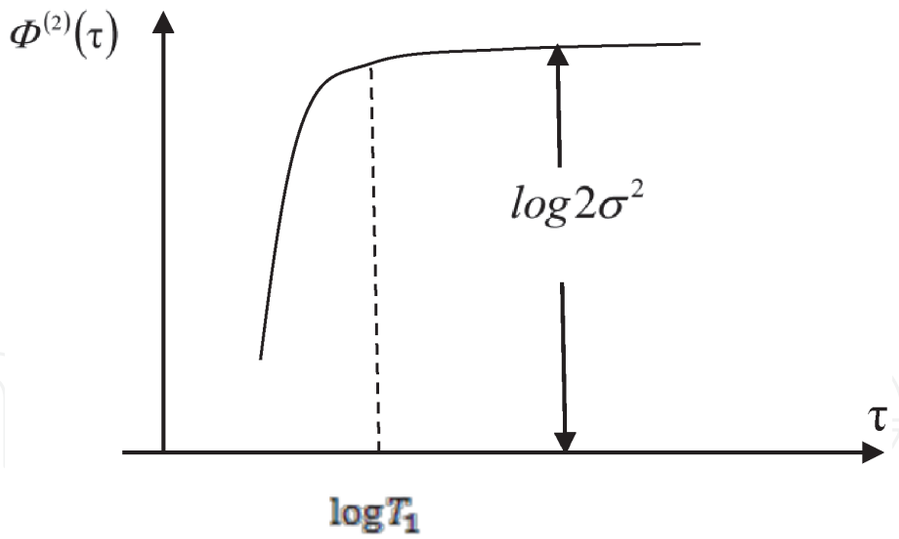

Figure 2.
Typical curve for function $\Phi^{(2)}(\tau)$, characterizing a chaotic signal $V(t)$ without a resonant component.

high-frequency $V_S(t)$ components. This method is built by analogy (**Figure 2**) with the solution of the diffusion equation and is based on the following "relaxation" procedure:

1. Set the value $V_1, \ldots, V_N$ of signal V with a step of discreteness Δt.

2. Calculate $\langle V \rangle = \frac{1}{N}\sum_{k=1}^{n} V(k)$ and put $V_{(R)} := V_{(k)} - \langle V \rangle, k = 1, \ldots, N$.

3. We calculate

$$\psi(m_\tau) = \frac{1}{N - m_\tau}\sum_{k=1}^{N-m_\tau} V_{(k)} V_{(k+m_\tau)}, \mathrm{m}_\tau = [\tau/\Delta \mathrm{t}] \tag{1}$$

where $\Phi^{(2)}(\tau) = 2[\psi(0) - \psi(\tau)], \sigma^2 = \psi(0),\ \tau = \mathrm{m}_\tau \cdot \Delta \mathrm{t}$

$$\mathrm{m}_\tau = 0, 1, \ldots, \mathrm{M} - 1, \mathrm{M} \in \mathrm{N} \tag{2}$$

4. We plot $\Phi^{(2)}(\tau)$ in bilogarithmic coordinates.

The asymptotic representation for $\Phi^{(2)}(\tau)$ is

$$\Phi^{(2)}(\tau) = \begin{cases} \tau^{2\mathrm{H}_1}, & if\, \tau << \mathrm{T}_1 \\ 2\sigma^2, & if\, \tau >> \mathrm{T}_1. \end{cases} \tag{3}$$

5. We take for T_1 the value τ, at which $\log \Phi^{(2)}(\tau)$ begins to stabilize to a constant equal to $\log(2\sigma^2)$.

6. Choose a sequence of small $\{\tau_k\}$ $(\mathrm{k} = 1, \ldots, \mathrm{k}_0\ \mathrm{k}_0 \approx 20), \tau_k << \mathrm{T}_1$, and construct a regression $\mathrm{y} = \mathrm{ax} + \mathrm{b}\ (\mathrm{b} = 0); \mathrm{y} = \ln \Phi^{(2)}(\tau), \mathrm{x} = ln\ \tau, \mathrm{a} = 2\mathrm{H}_1$.

According to the least squares method (LSM) estimate â, we calculate the estimate $\mathrm{H}_1 = \hat{\mathrm{a}}/2$.

7. We calculate

$$D = \frac{\sigma^2}{\Gamma^2(1 + H_1^*) \cdot T_1^*} \tag{4}$$

To calculate $\Gamma(x)$ for $x = 1 + H_1$, put $n = 10^3$and represent $\Gamma(x)$ in the form

$$\Gamma(x) = \frac{\Gamma(x+1)}{x} = \frac{\Gamma(x+2)}{x(x+1)} = \cdots = \frac{\Gamma(x+n)}{x(x+1)\cdot(x+nt)}. \tag{5}$$

The value $\Gamma(z)$ (we have $z = x + n$) is calculated by the formula

$$\Gamma(z) = exp\left\{\left(z - \frac{1}{2}\right) \ln z - z + \frac{1}{2}\, ln\, 2\pi\right\} \tag{6}$$

with an error of order $z^{-1} \approx 10^{-3}$ $n \approx 10^3$ $z = x + n$.

8. Denote by Δt and $\Delta\tau$ the steps of discreteness in t and τ, and

$$\omega = D \cdot \Delta\tau/(\Delta t)^2 \tag{7}$$

choose $\Delta\tau$ so that $\omega < 1/2$.

9. Put $M := N - 1$, and construct an iterative procedure according to $j = 0, 1, \ldots,$, according to which the value V_k^{j+1} at the jth step is calculated through the value V_k^j according to the formula

$$V_k^{j+1} = \omega V_{k+1}^j + \omega V_{k-1}^j + (1 - 2\omega) V_k^j \tag{8}$$

at $j = 0$ we set $V_k^j = V_{(k)}$; at $k = 1$ and $k = M$, the values of $V_k^{j+1}$are calculated by the formulas

$$V_1^{j+1} = (1 - 2\omega) V_1^j + 2\omega V_2^j, \quad V_M^{j+1} = (1 - 2\omega) V_M^j + 2\omega V_{M-1}^j. \tag{9}$$

The procedure stops at step $j = j_0$, in which.

$$\left|V_k^{j_0+1} - V_k^{j_0}\right| < \varepsilon, \text{ for } V_k = 1, \ldots, M, k = 1, 2, \ldots, N,$$

where ε is the given number (e.g., $\varepsilon = 10^{-m+1}$, where $10^{-m}$is the error in setting the initial values V_k).

10. The values $V_k^{j_0}$ determine the low-frequency component $V_R(t)$. Then $V(t) - V_R(t) = V_S(t)$ is the high-frequency component of the signal $V(t)$.

The described signal smoothing procedure is focused on minimizing the "high-frequency" information in the "low-frequency" part $V_R(t)$ of the signal and vice versa, minimizing the "low-frequency" information in the "high-frequency" part $V_S(t)$ of the signal. This conclusion follows from the diffusion nature of the partial differential equation used

$$\frac{\partial V}{\partial \tau} = \frac{\partial^2 V}{\partial t^2}, \tag{10}$$

represented as a difference equation

$$\frac{V_k^{j+1} - V_k^j}{\Delta\tau} = \frac{V_{k+1}^j + V_{k-1}^j - 2V_k^j}{(\Delta t)^2}, \tag{11}$$

corresponding to the simplest difference scheme for numerically solving Eq. (10). From (11) we obtain

$$V_k^{j+1} = V_k^j + \frac{\Delta\tau}{(\Delta t)^2}\left(V_{k+1}^j + V_{k-1}^j - 2V_k^j\right).$$

In notation $\omega = \Delta\tau/(\Delta t)^2$, the last equation is written in the form (8). From the theory of stability of difference schemes, it is known that this difference scheme will be absolutely stable at $\omega < 1/2$.

Such a relaxation procedure realizes the maximum rate of entropy generation and uses the relationship of entropy and Fisher information, which is a quantitative measure of the heterogeneity of the distribution density of the analyzed data array.

3. Parameterization of the singular component of the ECG signal

The procedure for parameterizing the singular part of the signal consists of the following sequence of steps [3]:

1. Let V(t) be represented as a sum

$$V(t) = V_R(t) + V_S(t).$$

2. Let $t_k = k\Delta t (k = 1, \ldots, N), t_0 = 0, t_N = T$ points of task $V(t)$ by $[0, T]$ with a certain step of discreteness Δt; $N = [T/\Delta t]$.

   We calculate the average value:

$$\langle V(t)\rangle = \frac{1}{N}\sum_{k=1}^{N} V(t_k) \tag{12}$$

   In what follows, we will assume that $\langle V(t)\rangle = 0$, i.e., signal $V(t)$, is stationary.

3. For stationary signal $V(t)$, the power spectrum $S(f)$ (Fourier transform of the autocorrelation function $\psi(\tau)$) coincides with $S_c(f)$ (cosine Fourier transform of $\psi(\tau)$).

   We set M from condition $\frac{4}{3} \le M \le N$ (in practice, take M close to N). We assume that M is an even number. For a time delay of $m_\tau = 0, 1, \ldots, M-1$, we calculate the autocorrelator:

$$\psi(m_\tau) = \frac{1}{N - m_\tau}\sum_{k=1}^{N-m_\tau} V(k)V(k + m_\tau) \tag{13}$$

4. Let $f = \frac{q/M}{\Delta t}$.

   We calculate the power spectrum $S(f) = S_c(f)$

$$S_c(f) = \frac{1}{\Delta t} S_c(q)$$

$$S_c(q) = \psi(0) + \psi\left(\frac{M}{2}\right)(-1)^q + 2\sum_{m=1}^{\frac{M}{2}-1} \psi(m)\cos\left(\frac{2\pi q m}{M}\right), \tag{14}$$

$$(q = 0, 1, \ldots, M-1)$$

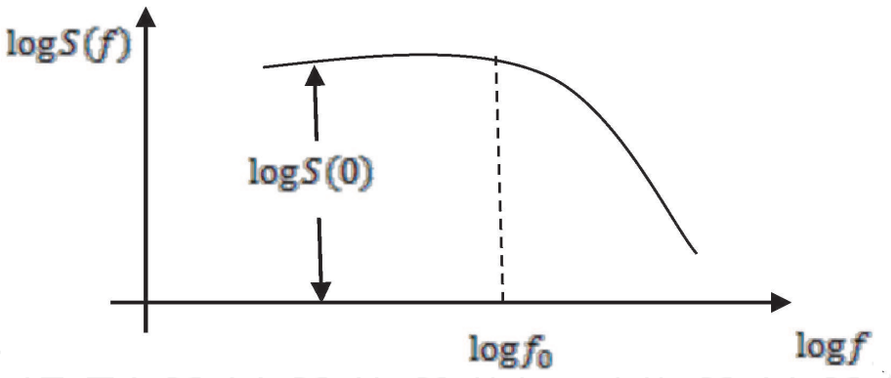

Figure 3.
Typical curve for function $S(f)$, characterizing a chaotic signal $V(t)$ without a resonant component.

5. We will construct the image $S(f)$ (or $|S(f)|$, if in some frequencies $S(f) < 0$) in a bilogarithmic scale (**Figure 3**).

   From **Figure 3** we find the frequency $f = f_0$, starting from which $S(f)$ ceases to stabilize around a certain constant $S(0)$.

6. Let $\left[f^*, \bar{f}^*\right]$ be the frequency interval in the region of the graph $S(f)$ (or $|S(f)|$), preceding the first strong peak of the power spectrum $S(f)$, corresponding to "irregularity-burst." We assume that $S(f)$ increases at $f \in \left[f^*, \bar{f}^*\right]$ and $S_s^*(0)$—a certain number from interval $\left[S(f^*), S\left(\bar{f}^*\right)\right]$.

7. We calculate the autocorrelator $\psi_{S,R}(\tau)$ according to the formula.

$$\psi_{S,R}(\tau) = \frac{1}{N - m_\tau} \sum_{k=1}^{N-m_\tau} [V_S(k)V_S(k+m_\tau) + V_R(k)V_S(k+m_\tau) + V_S(k)V_R(k+m_\tau)],$$
$$(m_\tau = 0, 1, \ldots, M-1) \tag{15}$$

8. We calculate the singular component $S_S(f)$ of spectrum $S(f)$ by the formula

$$S_S(f) = \frac{1}{\Delta t} S_S(q)$$
$$S_S(q) = \psi_{S,R}(0) + \psi_{S,R}\left(\frac{M}{2}\right)(-1)^q + 2\sum_{m=1}^{\frac{M}{2}-1} \psi_{S,R}(m) \cos\left(\frac{2\pi q m}{M}\right) \tag{16}$$
$$(q = 0, 1, \ldots, M-1)$$

9. For parameterization $S_S(f)$, we approximate this function by an interpolation expression:

$$\hat{S}_S(f) \approx \frac{S_S(0)}{1 + (2\pi f T_0)^{n_0}} \tag{17}$$

   Parameter T_0 by formula (17) will be determined by **Algorithm 1**, assuming that the "experimental" spectrum $S_S(f)$ is calculated by formula (16).

Algorithm 1.

9.1. Using the spectrum graph (**Figure 3**), we introduce the constants $f_0^*, \underline{f}^*, \overline{f}^*, S_S^*(0)$, as well as the threshold value $\mathrm{RSS}^* = 10^{10}$.

9.2. We set $S_S(0) = S_S^*(0)$ and evaluate the parameters T_0, n_0.

Build a regression

$$y = ax + b,$$

where

$$y = \ln\left|\frac{S_s(0)}{S_s(f)} - 1\right|, x = \ln 2\pi f, a = n_0, b = n_0 \ln T_0,$$

and estimate the coefficients a and b using the least squares method (least squares) for sample $\{y_m, x_m\}$ with y_m and x_m, corresponding to frequencies $f_m = \frac{m}{M \cdot \Delta t}$ $(m = 0, 1, \ldots, M-1)$.

We calculate the residual sum of squares

$$\mathrm{RSS}^{(1)} = \sum_{m=0}^{M-1} \left[y_m - \left(\hat{a}x_m + \hat{b}\right)\right]^2,$$

where â and $\hat{b}$ LSM are the estimations of parameters a and b.

If $\mathrm{RSS}^{(1)} < \mathrm{RSS}^*$, then $\mathrm{RSS}^* := \mathrm{RSS}^{(1)}$, $\hat{n}_0 = n_0^*$, $T_0^* = \hat{T}_0$, where $\hat{n}_0 = \hat{a}$, $\hat{T}_0 = exp\left\{\hat{b}/\hat{a}\right\}$.

9.3. We set $n_0 = n_0^*$, $S_S(0) = S_S^*(0)$and evaluate T_0.

Build a regression

$$y = ax + b(b = 0),$$

where

$$y = \left|\frac{S_s(0)}{S_s(f)} - 1\right|^{1/n_0}, x = 2\pi f, a = T_0.$$

We calculate $\mathrm{RSS}^{(2)} = \sum_{m=0}^{M-1} \left[y_m - \hat{a}x_m\right]^2$.

If $\mathrm{RSS}^{(2)} < \mathrm{RSS}^*$, then $\mathrm{RSS}^* := \mathrm{RSS}^{(2)}$ and $T_0^* = \hat{T}_0$, where $\hat{T}_0 = \hat{a}$.

9.4. We set $T_0 = T_0^*$, $n_0 = n_0^*$ and evaluate $S_S(0)$.

Build a regression

$$y = ax + b(b = 0),$$

where

$$y = S_s(f), x = \frac{1}{1 + (2\pi f\, T_0)\, n_0}, \quad a = S_S(0)$$

We calculate $RSS^{(3)} = \sum_{m=0}^{M-1} \left[y_m - \hat{a}x_m\right]^2$.

If $RSS^{(3)} < RSS^*$, then $RSS^* := RSS^{(3)}$, $S_S(0) = \hat{S}_S(0)$, where $\hat{S}_S(0) = \hat{a}$.

9.5. We set $S_S(0) = S_S^*(0)$, $T_0 = T_0^*$ and evaluate n_0.

Build a regression

$$y = ax + b(b = 0),$$

where

$$\mathrm{y} = ln\left|\frac{\mathrm{S_s}(0)}{\mathrm{S_s}(\mathrm{f})} - 1\right|, \mathrm{x} = ln\,(2\pi \mathrm{f T_0}), \mathrm{a} = \mathrm{n_0}.$$

We calculate $RSS^{(4)} = \sum_{m=0}^{M-1} \left[\mathrm{y}_m - \hat{\mathrm{a}}\mathrm{x}_m\right]^2$.

If $RSS^{(4)} < RSS^*$, then $\mathrm{n}_0^* = \hat{\mathrm{n}}_0$, where $\hat{\mathrm{n}}_0 = \hat{\mathrm{a}}$.

As a result of **Algorithm 1**, we obtain the three parameters $S_S(0) = S_S^*(0)$, $n_0 = n_0^*$, $T_0 = T_0^*$, characterizing the interpolation expression (17) for the singular component of the spectrum $S_S(f)$.

4. Informative diagnostic parameters of the singular component of the ECG signal

During a computational experiment, electrocardiographic signals with a normal state of the cardiovascular system and pathological signals ("tachycardia," "arrhythmia," and "atrial fibrillation") were analyzed. We used data from the public site www.PhysioNet.org for the II standard lead. The ECG removal parameters (type of lead, sampling frequency, time, number of samples, and signal amplitude) are included in the sample. The sampling rate for various samples varies from 125 to 1000 Hz. The values of the presented samples, taking into account the sign discharge, correspond to the use of a 12-bit ADC.

In **Figures 4–6**, the graphs of the spectral power of the ECG signal for the norm, the singular component of this signal, and the estimation of the singular component of this signal are presented.

In **Figures 7–9**, as an example, similar relationships for an ECG signal with a range of "atrial arrhythmia" are presented.

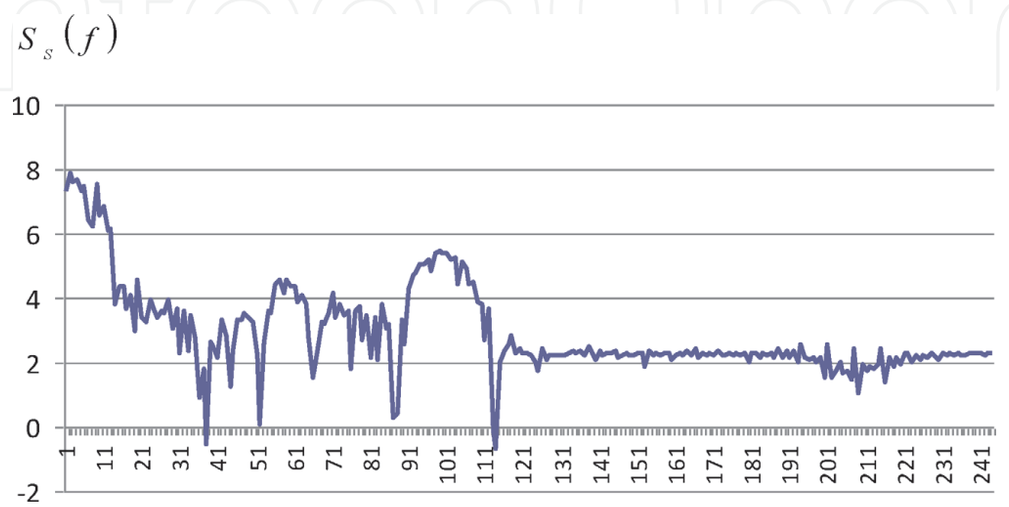

Figure 4.
Graphs of the spectral power of the ECG signal for the norm.

$S_S(0)$

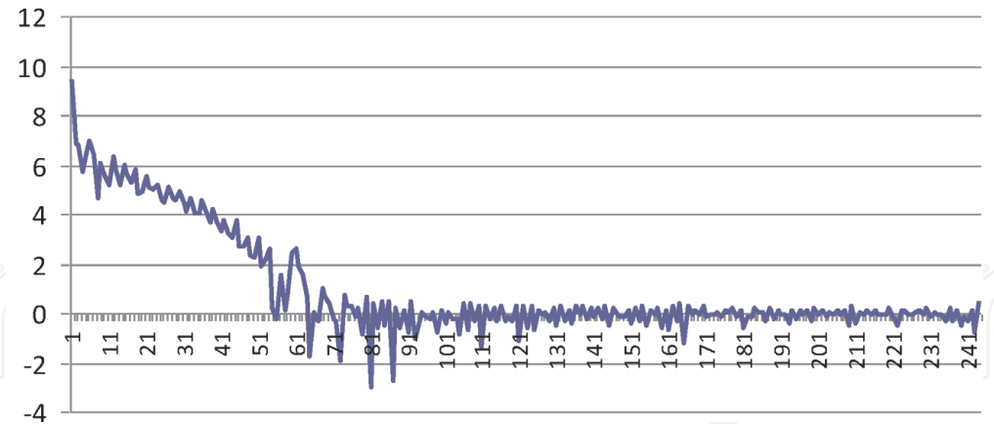

Figure 5.
Graphs of the singular component of this signal.

$\hat{S}_S(0)$

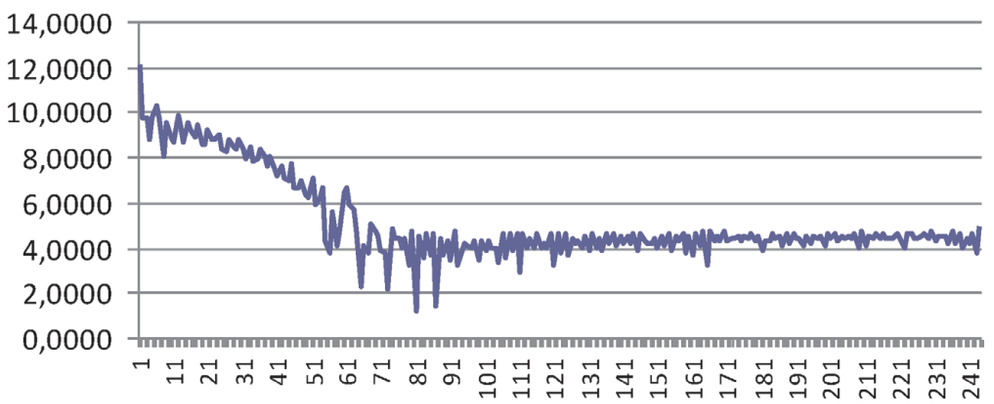

Figure 6.
Graphs of the estimation of the singular component of this signal.

$S_S(f)$

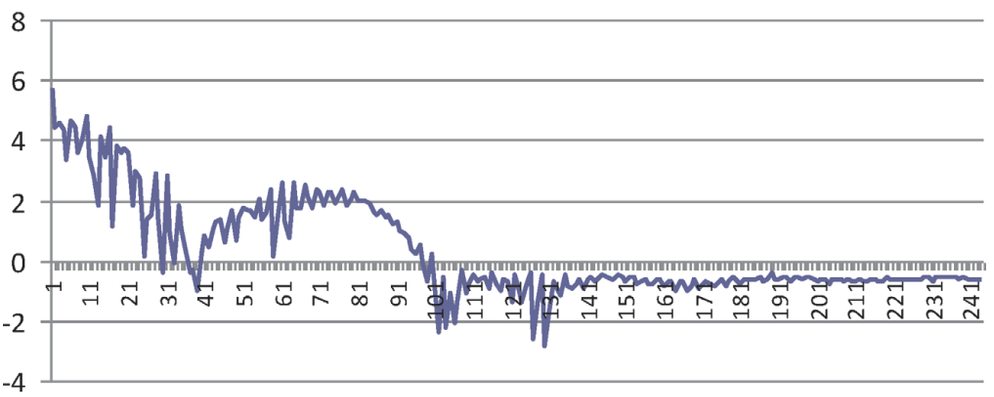

Figure 7.
Graphs of the spectral power of the ECG signal for the "atrial arrhythmia."

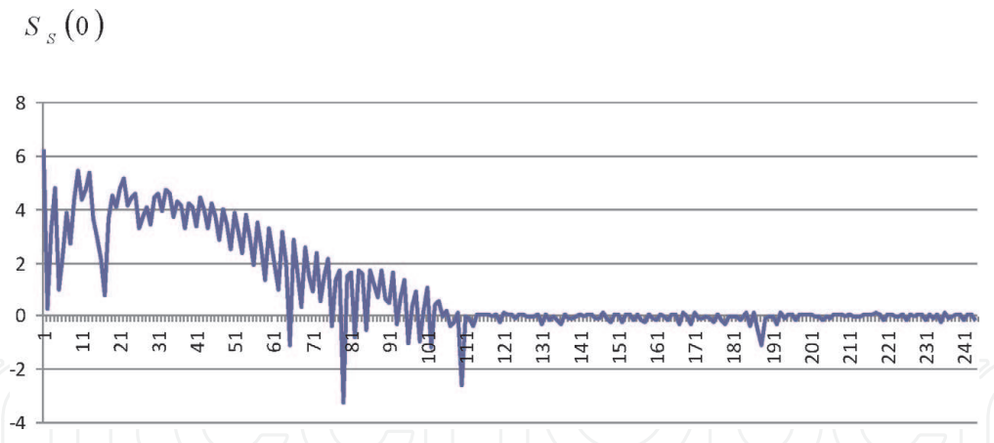

Figure 8.
Graphs of the singular component of the "atrial arrhythmia."

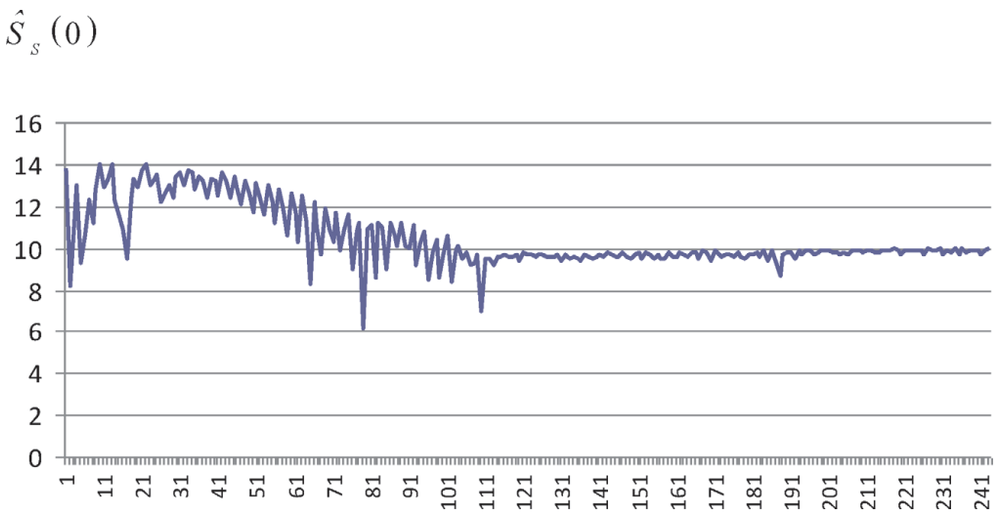

Figure 9.
Graphs of the estimation of the singular component of the "atrial arrhythmia."

For all the considered states of the cardiovascular system, the same dependencies were obtained, and based on the obtained dependencies, informative parameters of the singular component of the ECG signals were calculated (**Table 1**).

The high specificity of $S(f)$ patterns obtained in the study of the cardiovascular system in the norm with the indicated pathologies can be used to diagnose diseases. Dependence $S(f)$ built on the basis of different ECGs and the corresponding informative parameters obtained by them differ from each other, which gives

ECG signal	n_0	T_0	$S_s(0)$
Norm	0.3414	0.0042	437.8090
Atrial fibrillation	0.3836	0.0036	334.3640
Ventricular tachycardia	0.4123	0.0032	197.3580
Atrial arrhythmia	0.4013	0.0059	43.7105

Table 1.
Informative parameters of the singular component of ECG signals.

reason to consider these dependencies as patterns characterizing the condition of the patient under study. The obtained informative parameters can be considered as distinguishing features for the differential diagnosis of cardiovascular diseases (e.g., using artificial neural networks).

This approach shows the possibility of flicker-noise spectroscopy as a method that allows you to establish significant differences in the original, visually not very different, ECG signals.

5. Parameterization of the regular part of the ECG signal and determination of informative diagnostic parameters

The determination of the parameters of a chaotic signal given on a limited interval T is set on the basis of the flicker-noise spectroscopy method, taking into account the contributions of the "resonant components" to the autocorrelation function [4].

$$\Psi(\tau) = \langle V(t), V(t+\tau) \rangle, \tag{18}$$

and, therefore, to cosine conversion

$$S_c(f) = \int_{-T/2}^{T/2} \Psi(\tau) \cos(2\pi f \tau) d\tau \tag{19}$$

and second-order difference moment

$$\Phi^{(2)}(\tau) = \left\langle \left| V(t) - V(t+\tau|^2 \right\rangle. \tag{20}$$

Here $V(t)$ is a stationary signal ($\langle V(t) \rangle = 0$), and $\langle \cdot \rangle$ is a symbol of the average value.

The developed method of signal parametrization is based on the fact that the introduced "irregularities-bursts" and "irregularities-jumps" contribute to various spectral regions of dependence $S(f)$.

In fact, the first step in the parameterization of irregularities was to isolate the "burst" (singular), most "high-frequency" (the so-called "flicker-noise tail") component of the signal irregularities in the spectral dependence $S(f)$.

Based on the remaining (after subtracting the "burst" contribution) spectral dependence, we can now determine the structure function $\Phi^{(2)}(\tau)$, which contains the contributions from the "jump" and "resonance" components that slowly change against its background. The next steps are to parameterize the "higher frequency" (of those remaining) "hopping" (regular) component using the least squares method.

It must be borne in mind that when solving the signal parametrization problem under consideration, problems arise due to the limited averaging interval T. For this reason, in particular, it is the "experimental" dependence $V(t)$ constructed on the basis of observed signal $S(f)$ that may turn out to be negative in some frequency intervals. Therefore along with four in such cases, $S(f)$ is introduced into consideration.

The procedure for parameterizing the regular part of the signal is presented below in the form of the following sequence of operations:

1. From the extreme spectrum $S(f)$, we subtract the singular component $S_s(f)$ calculated by the interpolation formula (we denote the result by $S_{rR}(f)$)

$$S_{rR}(f) = S(f) - S_s(f) \tag{21}$$

The resulting difference characterizes the contribution of the "resonant" components $S_r(f)$ and the "irregularities-jumps" $S_R(f)$ to the general dependence $S(f)$. If it turns out that $S_{rR}(f) < 0$ in some frequency intervals, we assume $S_{rR}(f) := |S_{rR}(f)|$.

2. Take the inverse cosine Fourier transform of $S_{rR}(f)$

$$\psi_{rR}(\tau) = 2\int_0^{f_{max}} S(f)\cos(2\pi f\tau)df, (\tau \le \tau^* = T/4) \tag{22}$$

$$f_{max} = \frac{1}{4\Delta t}, \tau = k\cdot\Delta\tau(k = 1, \ldots, k_0), \Delta\tau = \frac{T/4}{k_0}, k_0 = 500.$$

Put $a = 0, b = f_{max}, h = f_{max}/n, n = 100$, $S_{rR}(f)\cdot\cos(2\pi f\tau) = g(f,\tau)$ and apply the trapezoid formula:

$$\int_a^b g(f,\tau)df = h\left(\frac{g(a,\tau)}{2} + g(a+h,\tau) + g(a+2h,\tau) + \ldots + g(b-h,\tau) + \frac{g(b,\tau)}{2}\right)$$

3. We calculate

$$\Phi_{rR}^{(2)}(\tau) = 2[\psi_{rR}(0) - \psi_{rR}(\tau)], \tau = k\cdot\Delta\tau(k = 1, \ldots, k_0)$$

4. Put $\tilde{\Phi}_r^{(2)}(\tau) = \tilde{\Phi}_{rR}^{(2)}(\tau)$.
5. We denote

$$\tilde{\Phi}^{(2)}(\tau) = \Phi_r^{(2)}(\tau) + \Phi_R^{(2)}(\tau). \tag{23}$$

where $\Phi_R^{(2)}(\tau)$ is given by the interpolation formula:

$$\Phi_R^{(2)}(\tau) = \begin{cases} 2\sigma_1^2\cdot\dfrac{1}{\Gamma^2(H_1+1)}\left(\dfrac{\tau}{T_1}\right)^{2H_1}, \ \tau << T_1, \\ 2\sigma_1^2\left[1 - \Gamma^{-1}(H_1)\left(\frac{\tau}{T_1}\right)^{H_1-1} exp\left(-\frac{\tau}{T_1}\right)\right]^2 \end{cases} \tag{24}$$

6. Compare the experimental structural function $\Phi^{(2)}(\tau)$, determined by the formula

$$\Phi^{(2)}(\tau) = 2[\psi(0) - \psi(\tau)], \tag{25}$$

where

$$\psi(m_\tau) = \frac{1}{N - m_\tau}\sum_{k=1}^{N-m_\tau} V_{(k)}V_{(k+m_\tau)} \tag{26}$$
$$m_\tau = [\tau/\Delta t]$$

with function $\Phi^{(2)}(\tau)$ determined by formula (20) using the least squares method.

- We set $RSS^* = 10^{10}$, $T_1 = T_1^*$
- A preliminary estimate T_1^* of parameter T_1 can be obtained using the asymptotic representation of structure function $\Phi^{(2)}(\tau)$ (**Figure 10**).

The value $\Phi^{(2)}(\tau)$ is taken as T_1^* for small delays, at which $\Phi^{(2)}(\tau) \approx 2\sigma^2$ takes the maximum value $\Phi^{(2)}(\tau) \approx 2\sigma^2$.
We estimate parameters σ_1, H_1 at $\tau << T_1$.
Build a regression

$$y = ax + b,$$

where

$$y = \ln\left\{\Phi^{(2)}(\tau) - \Phi_r^{(2)}\right\}, x = \ln\left\{\frac{\tau}{\tau_1}\right\}, a = 2H_1, b = 2\ln\frac{\sigma_1}{\Gamma^2(H_1+1)}.$$

LSM-estimates $\hat{a}$ and $\hat{b}$ are obtained on the basis of sequence $\{\tau_k\}$, $(k = 1, \ldots, k_1)$ close to $\tau = 0$, using representation (21) for $\hat{\Phi}^{(2)}(\tau)$.
We calculate

$$\mathrm{RSS}^{(1)} = \sum_{k=1}^{k_1}\left[\mathrm{y}_k - (\hat{\mathrm{a}}\mathrm{x}_k + \mathrm{b})\right]^2,$$

- where y_k and x_k correspond to delays τ_k.
- If $RSS^{(1)} \geq RSS^*$, then go to Section 6.5.
- Otherwise, set $RSS^* := RSS^{(1)}$, $\sigma_1^* = \hat{\sigma}_1$, and $\mathrm{H}_1^* = \hat{H}_1$, where $\hat{\mathrm{H}}_1 = \frac{\hat{a}}{2}$ and $\hat{\sigma}_1 = \Gamma^2\left(\hat{H}_1 + 1\right)\exp\left\{\hat{b}/2\right\}$.

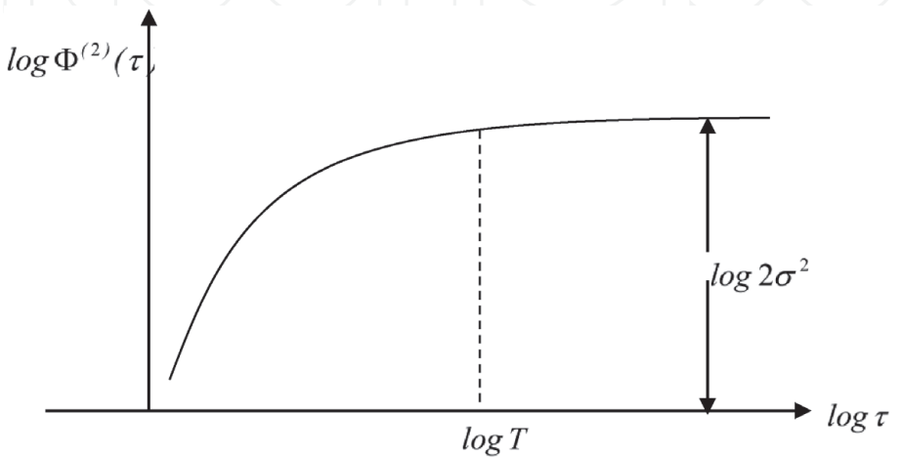

Figure 10.
Graph of function $\Phi^{(2)}(\tau)$ in bilogarithmic coordinates.

- Given $\sigma_1 = \sigma_1^*$, we estimate H_1, T_1 at $\tau << T_1$
- Build a regression

$$y = ax + b(b \neq 0),$$

- where $a = 2H_1, b = -\ln\Gamma^2(H_1+1) - 2H_1 \ln T_1, y = \ln\left\{\frac{\Phi^{(2)}(\tau)-\Phi_r^{(2)}}{2\sigma_1^2}\right\}, x = \ln\tau.$
- LSM grades $\hat{a}$ and $\hat{b}$ are obtained by sequence $\{\tau_k\}, (k = 1, \ldots, k_1)$.
- We calculate

$$RSS^{(2)} = \sum_{k=1}^{k_1}\left[\mathrm{y}_k - \left(\hat{\mathrm{a}}\mathrm{x}_k + \hat{\mathrm{b}}\right)\right].$$

- If $RSS^{(2)} \geq RSS^*$, then go to Section 6.5.
- Otherwise, set $\mathrm{H}_1^* = \hat{H}_1, \mathrm{T}_1^* = \hat{\mathrm{T}}_1$, where $\hat{\mathrm{H}}_1 = \frac{\hat{a}}{2}, \hat{T}_1 = \left\{\Gamma^2(H_1+1)\right\}^{-\frac{1}{2H_1}} \exp\left\{-\frac{b}{2H_1}\right\}$.
- Given $\sigma_1 = \sigma_1^*, H_1 = \mathrm{H}_1^*$, we estimate T_1 at $\tau << T_1$.
- Build a regression

$$y = ax + b(b = 0),$$

where

$$y = \ln\left\{\frac{\Phi^{(2)}(\tau) - \Phi_r^{(2)}(\tau)}{2\sigma_1^2/\Gamma^2(H_1+1)}\right\}, x = \tau, a = \frac{1}{T_1}.$$

- In LSM, a score of $\hat{a}$ will be obtained by sequence $\{\tau_k\}$, $(k = 1, \ldots, k_1,\ k_1 << k_0)$.
- We calculate $T_1 = 1/\hat{a}$
- We calculate $RSS^{(3)} = \sum_{k=1}^{k_1}\left[\mathrm{y}_k - \hat{\mathrm{a}}\mathrm{x}_k\right]^2$.
- If $RSS^{(3)} \geq RSS^*$, then go to Section 6.5.
- Otherwise, we set $RSS^* = RSS^{(3)}, \mathrm{T}_1^* = \hat{\mathrm{T}}_1$.
- Given $H_1 = \mathrm{H}_1^*, T_1 = \mathrm{T}_1^*$, we estimate σ_1 at $\tau >> T_1$.
- Build a regression

$$y = ax + b(b = 0),$$

- where $y = \Phi^{(2)}(\tau) - \Phi_r^{(2)}$, $x = \left[1 - \Gamma^{-1}(H_1)\left(\frac{\tau}{T_1}\right)^{H_1-1} \exp\left\{-\frac{\tau}{T_1}\right\}\right]^2$, $a = 2\sigma_1$.
- We calculate the least squares method (LSM) estimation by sequence $\{\tau_k\}$, $\tau_k = T - k \ \ (k = 1, \ldots, k_1)$.
- We calculate $\hat{\sigma}_1 = \sqrt{\hat{a}/2}$.
- We calculate $RSS^{(4)} = \sum_{k=1}^{k_1} \left(y_k - \hat{a}x_k\right)^2$.
- If $RSS^{(4)} > > RSS^*$, then go to Section 6.5.
- Otherwise, we set $RSS^* = RSS^{(4)}$, $\sigma_1^* = \hat{\sigma}_1$.
- 6.5. Suppose RSS^*, σ_1^*, H_1^*, T_1^*.
- As a result of the proposed algorithm, we obtain the three parameters $\sigma_1 = \sigma_1^*$, $H_1 = H_1^*$, and $T_1 = T_1^*$, characterizing the interpolation expression (21) for $\Phi_R^{(2)}(\tau)$.

6. Informative diagnostic parameters of the regular component of the ECG signal

Using the above algorithm, we obtained the graphs of functions $\Phi^{(2)}(\tau)$ in bilogarithmic coordinates for the normal state of the cardiovascular system and a number of "catastrophic" arrhythmias (ventricular tachycardia, atrial fibrillation, atrial arrhythmia). An example is given of such a dependence for the state of the cardiovascular system—"ventricular tachycardia" (**Figure 11**) and atrial arrhythmia

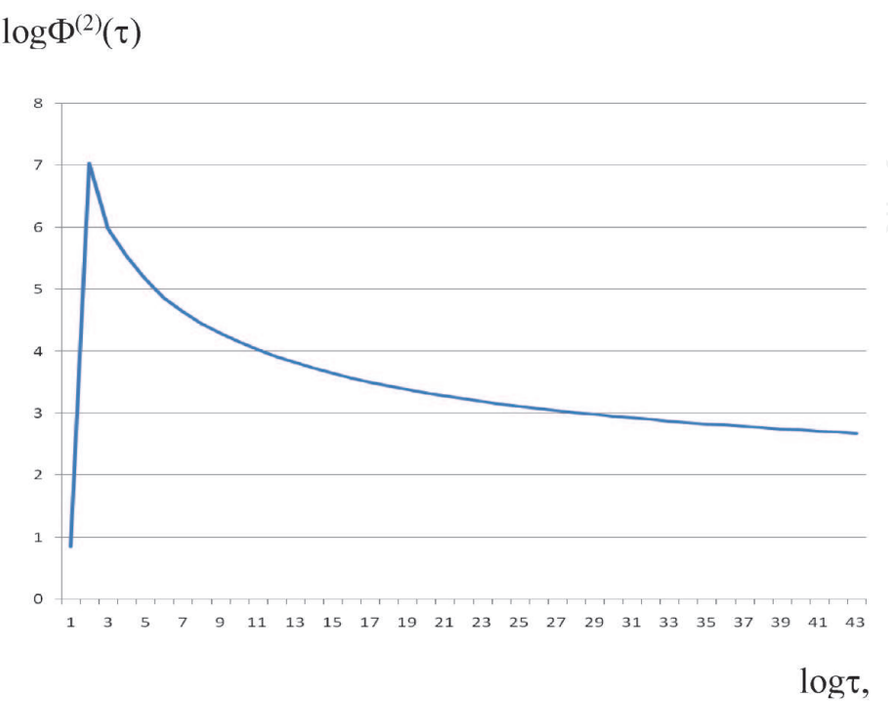

Figure 11.
Dependence $\log\Phi^{(2)}(\tau)$ for ventricular tachycardia.

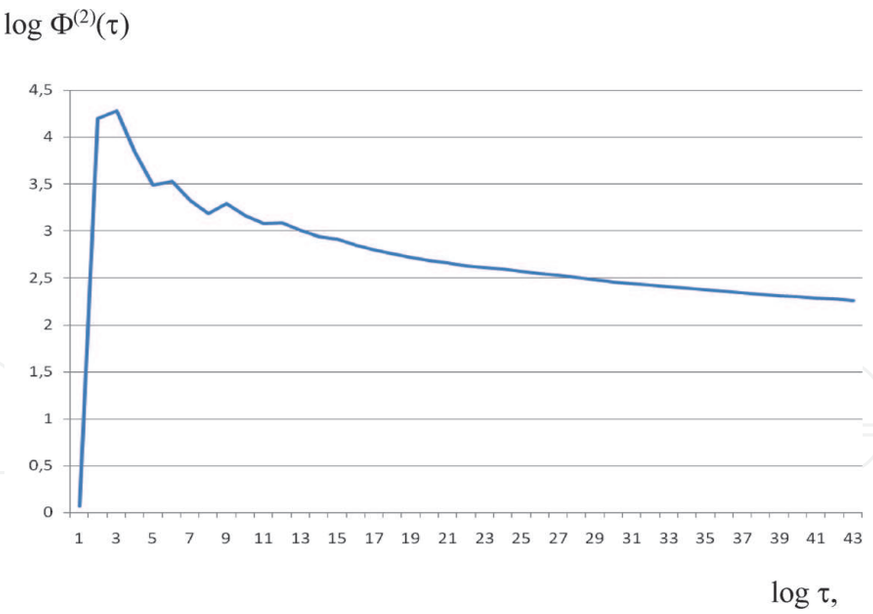

Figure 12.
Dependence $\log\Phi^{(2)}(\tau)$ for atrial rhythm.

No.	ECG signal	σ_1	H_1	T_1
1	Norm	0.55	11.133	15.080
2	Atrial fibrillation	0.435	11.388	0.0640
3	Ventricular tachycardia	0.51	10.913	0.6840
4	Atrial arrhythmia	0.208	11.298	11.560

Table 2.
Informative parameters of the regular component.

(**Figure 12**). When conducting a computational experiment, we used the experimental data from the publicly available website www.PhysioNet.org.

For the considered conditions of the cardiovascular system, on the basis of the obtained dependencies, the informative parameters of the regular component of the ECG signals were calculated (**Table 2**).

Thus, for the considered functional conditions of the cardiovascular system, three informative parameters $n_0, T_0, S_s(0)$ for the singular component of the ECG signal and three informative diagnostic parameters σ_1, H_1, T_1 for the regular component of the ECG signal were obtained by flicker-noise spectroscopy.

A complex of six diagnostic parameters can be used to diagnose catastrophic conditions of the cardiovascular system (e.g., using an artificial neural network, where these parameters are considered as input data).

7. Fluctuation dynamics of electrocardiograms and the choice of sampling frequency of the studied signals

In the general case, when analyzing a complex chaotic signal measured at a certain sampling frequency f_d, a set of the indicated parameters is determined that characterizes the correlation interconnections in the sequences of irregularities-jumps and irregularities-bursts characteristic of a given signal determined with a sampling frequency of f_d. Thus, one of the main factors allowing to realize the allocation of the contribution of irregularities to the analyzed real signals is the

No.	ECG signal	Singular component			Regular component		
		$S_s(0)$	T_0	n_0	σ_1	H_1	T_1
1	Norm	437.80	0.0042	0.3414	0.55	11.133	15.080
2	Ventricular tachycardia	197.358	0.0032	0.4123	0.51	10.913	0.6840
3	Atrial fibrillation	334.364	0.0036	0.3836	0.435	11.388	0.0640
4	Atrial Arrhythmia	43.7105	0.0059	0.4013	0.208	11.298	11.560

Table 3.
Informative diagnostic parameters for various functional conditions of the cardiovascular system.

f_d, Hs	N	Singular component			Regular component			$\frac{4S(0)}{N}$
		$S_s(0)$	T_0	n_0	σ_1	H_1	T_1	
500	29.859	437.80	0.0042	0.3414	0.55	11.133	15.080	0.05
250	14.930	403.72	0.0028	0.4187	0.5044	10.845	1.38	0.08

Table 4.
Norm.

f_d, Hs	N	Singular component			Regular component			$\frac{4S(0)}{N}$
		$S_s(0)$	T_0	n	σ_1	H_1	T_1	
500	29.859	197.358	0.0032	0.4123	0.5180	10.913	0.6840	0.026
250	14.930	175.80	0.0034	0.3446	0.517	15.200	0.340	0.10

Table 5.
Ventricular tachycardia.

variation of the used frequencies f_d. If the analyzed time series is obtained at a sufficiently high sampling frequency f_d, then the analysis of dependencies $\Phi^{(2)}(\tau)$ and $S(f)$, calculated on the basis of time series obtained from the initial time series with a decreasing sampling frequency, allows us to estimate the measure of "stability" of parameters σ_1, T_1 and H_1 (for $\Phi^{(2)}(\tau)$) and the measure of variability of parameters $S_s(0), T_0$ and n_0 (for $S(f)$).

The high specificity of dependencies $\Phi^{(2)}(\tau)$ and $S(f)$ obtained by analyzing the state of complex systems can be used to diagnose diseases, as well as a combination of these parameters for their classification. We analyzed the four types of ECG signals—normal and cardiac "catastrophic" arrhythmias that directly threatened the patient's life, ventricular tachycardia, atrial fibrillation, and atrial arrhythmia. To identify the characteristics of the analyzed signals, it is necessary to evaluate the entire set of digitized data of $V(t)$ electrocardiograms for the indicated states of the cardiovascular system. When conducting the computational experiment, the experimental data from the public site www.PhysioNet.org were used.

The signals were taken from the II standard lead for ~60 s with a sampling frequency of f_d = 500 Hs and containing N = 29,859 values. Thus, a time series of ECG signals was obtained at a sufficiently high sampling frequency of f_d, since it can be used to obtain a set of new time series at sampling frequencies of less than f_d times.

The results of the corresponding analysis for the indicated functional conditions of the cardiovascular system at a sampling frequency of ECG signals f_d = 500 Hs are shown in **Table 3**.

We will carry out a comparative analysis of informative parameters for the two states of the cardiovascular system: normal (**Table 4**) and ventricular tachycardia (**Table 5**) for sampling frequencies f_d = 500 Hs and f_d = 250 Hs.

From the obtained tables, it follows that with increasing sampling frequency f_d, the high-frequency contribution to the power spectrum $S(f)$ increases due to the inclusion of "bursts" in the analyzed signal corresponding to the increased frequency f_d. In this case, changes in dependence $\Phi^{(2)}(\tau)$ also occur at small τ, which are caused by the contribution of local changes in the values of the "laminar" signal sections. Therefore, with an increase of f_d, parameters T_0 and n_0, characterizing the high-frequency region of dependence $S(f)$, and parameters H_1 and T_1, characterizing the dependence of $\Phi^{(2)}(\tau)$ for small τ, change. The value of parameter σ_1 and the nature of spectral dependence $S(f)$ change to a much lesser extent. Small variations in the standard deviation parameter σ_1 indicate a smaller dependence of function $\Phi^{(2)}(\tau)$ on f_d. At the same time, the signal analysis in flicker-noise spectroscopy reveals the dynamics of changes in parameters H_1 and T_1 at small τ, as well as parameters T_0 andn_0, characterizing dependence $S(f)$ in the high-frequency region. Since dependence $S(f)$ is determined by the number of M terms in a discrete expression for $S(f)$, it is convenient to use normalized expressions obtained by multiplying $S(f)$ by a factor of $1/M = 4/N$ when changing the sampling frequencies. With this normalization, functional differences in dependence $S(f)$, due to the use of signals measured at different sampling frequencies, are detected more explicitly.

Thus, when analyzing a complex chaotic signal during flicker-noise spectroscopy, a set of parameters is determined that characterize the correlation relationships in the sequences of irregularity-jumps and irregularity-bursts characteristic of this signal, determined with a sampling frequency of f_d. The analysis of dependencies $\Phi^{(2)}(\tau)$ and $S(f)$, calculated on the basis of time series with decreasing sampling frequency, allows you to evaluate the measure of "stability" of parameters σ_1, T_1, and H_1, determined on the basis of $\Phi^{(2)}(\tau)$, and the measure of variability of the parameters $S_s(0), T_0$, and n_0, concerning dependence $S(f)$.

8. The use of neural network technology in flicker-noise spectroscopy of an electrocardiogram

Based on a computational experiment, dependencies were obtained for the normal state of the cardiovascular system and a number of "catastrophic" arrhythmias (ventricular tachycardia, atrial fibrillation, atrial arrhythmia). We used the experimental data from the public website www.PhysioNet.org.

As a result of analyzing the power spectrum $S(f)$, informative parameters were obtained for the singular component of the ECG signal: T_0, determining some characteristic time within which the measured dynamic variable is interconnected $V(t_i)$; n_0, dimensionless parameter that effectively determines how this relationship is lost as frequencies decrease to $1/2\pi T_0$; and $s(0)$, contribution to the power spectrum $S(f)$, determined by the most high-frequency singular component [5].

The parameterization of the regular component of the ECG signal is carried out using expression $\Phi^{(2)}(\tau)$ with parameters T_1, τ_1, and H_1. In this case, parameter T_1 determines the characteristic time at which the values of the dynamic variables $V(t_i)$ do not correlate. To obtain reliable values of variance σ_1^2, it is necessary to calculate it at time intervals exceeding T_1. In this case, parameter H_1 shows by what law the relationship between the quantities $V(t_i)$ measured at different time instants is lost—the Hurst exponent.

Thus, when analyzing a complex chaotic signal, which is an ECG signal, we consider a set of six parameters, characterizing the correlation relationships in the sequences of irregularities—"jumps" and irregularities—"bursts" inherent in this signal.

9. The choice of artificial neural network and its characteristics

The obtained values of the parameters of the singular and regular component of the ECG signals can be used for differential diagnosis of the functional state of the cardiovascular system using artificial neural networks, where these parameters are considered as input data.

For the computational experiment, a perceptron three-layer network with direct connections was chosen (**Figure 13**).

To train the neural network, the backpropagation algorithm was used. The training time was about 240 s, the maximum network error was about 0.05, and the degree of training was about 0.01.

To recognize the pathologies of the cardiovascular system, a modular version of the structure of the construction of neural network blocks can be used (**Figure 14**).

The structure includes several parallel neural network modules, built on the basis of the structure of a multilayer perceptron. The advantage of this structure is the concentration of resources of each module on the recognition of only one pathology, which helps to reduce the likelihood of an error in the wrong conclusion for the whole system. In addition, the functionality of an artificial neural network is expanded by increasing the number of neural network modules to recognize new pathologies without retraining the entire system.

The main factor that allows one to distinguish the contribution of irregularities to the analyzed electrocardiographic signals is the variation of the used sampling frequencies f_d of the real signal. An analysis of the dependencies of the power spectrum and the second-order difference moment calculated on the basis of time series with a varying sampling frequency makes it possible to evaluate the measure of "stability" for the regular component and between the "variability" of its informative parameters for the singular component. In this case, parameter f_d can be used as an additional input parameter of an artificial neural network for recognition of the state of the cardiovascular system.

The presentation of electrocardiographic signals in the form of successive irregularities allows the use of flicker-noise spectroscopy in the analysis of such signals. The chaotic signal represented by the time series during flicker-noise spectroscopy allows one to parameterize these signals and determine informative diagnostic

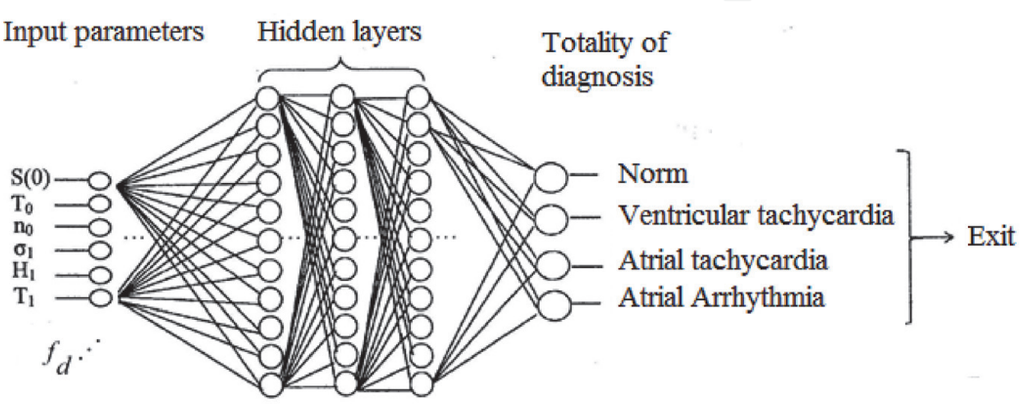

Figure 13.
The structural diagram of the proposed artificial neural network.

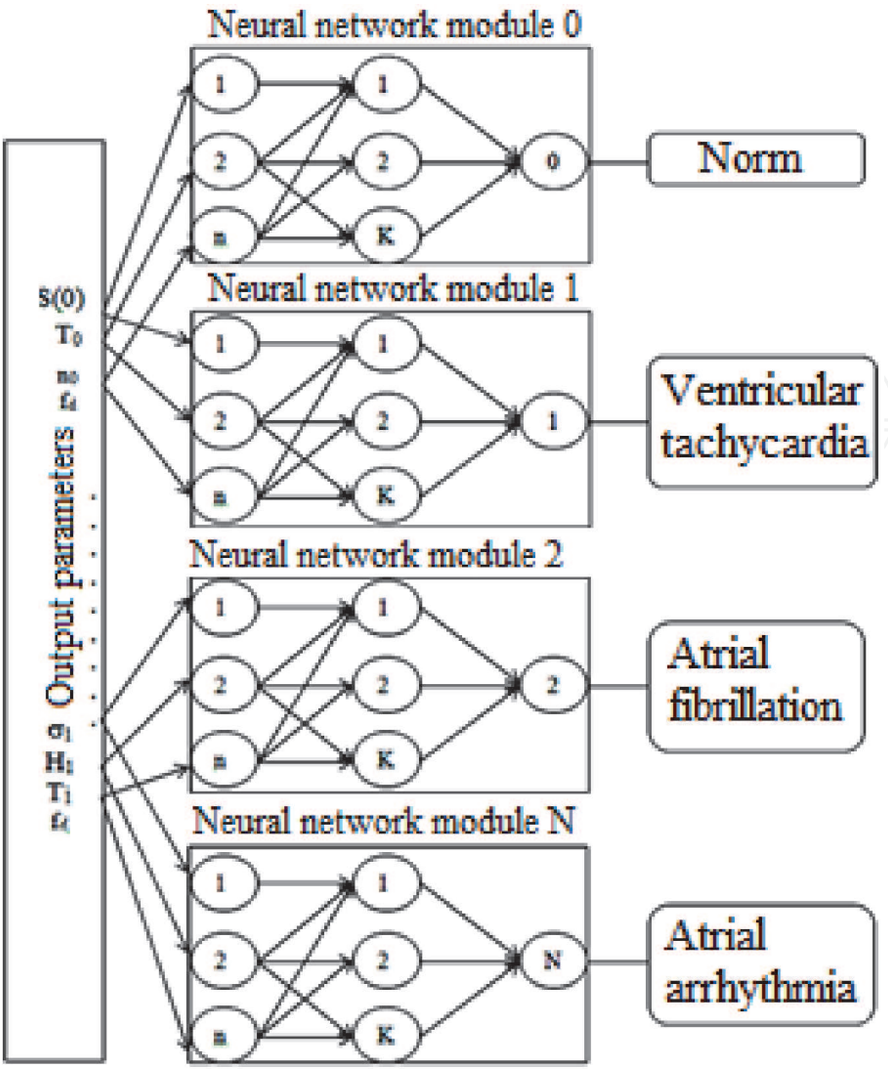

Figure 14.
A modular version of the construction of a neural network for recognition of pathologies (the number of input parameters, the number of neurons in the intermediate layer, the number of pathologies analyzed).

parameters, characterizing the functional state of the cardiovascular system. The set of informative parameters, as well as the sampling frequency of the signal, which determines the dynamics of changes in these parameters, allows the classification of heart diseases using a neural network.

Author details

Abdullayev Namiq Tahir* and Ahmadova Khadija Ramiz*
Department of Biomedical Engineering, Azerbaijan Technical University, Baku, Azerbaijan

*Address all correspondence to: a.namik46@mail.ru and phd.khadija@gmail.com

References

[1] Timashev SF. Flicker-Noise Spectroscopy: Information in Chaotic Signals. Moscow: FIZMATLIT; 2007. p. 248. (in Russia)

[2] Timashev SF, Polyakov YS. Review of flicker noise spectroscopy in electrochemistry. Fluctuation and Noise Letters. 2007;**7**(2):R15-R47

[3] Abdullaev NT, Dyshin OA, Gasankulieva MM. Flicker noise spectroscopy of electrocardiographic signals. Biomedical Engineering. 2016; **49**(5):268-273

[4] Abdullaev NT, Dyshin OA, Gasankulieva MM. Parameterization of the regular component of the ECG signal for diagnosis of the critical states of the cardiovascular system. Biomedical Engineering. 2016;**50**(3): 166-169

[5] Abdullaev NT, Gasankulieva MM, Dzhabieva ID. Application of neural network technology in flicker-noise spectroscopy of electrocardiograms. Information Technologies. 2018;**6**: 02-405 (in Russia)